Stainless steel 316L–hydroxyapatite composite via powder injection moulding: rheological and mechanical properties characterisation

M. I. Ramli*[1], A. B. Sulong[1], N. Muhamad[1], A. Muchtar[1] and A. Arifin[1,2]

Powder injection moulding is a manufacturing process capable of producing complex, precise and net-shaped components from metal or ceramic powders at a competitive cost. This study investigated the rheological properties of stainless steel 316L–hydroxyapatite composite by using palm stearin and polyethylene as a binder system, evaluates the physical and mechanical properties, and composition change of the sintered part at different temperatures through powder injection moulding process. Stainless steel 316L powder was mixed with hydroxyapatite by adding a binder system (palm stearin and polyethylene) at 58·0 vol% powder loading prepared via critical powder volume percentage. A green dumbbell-shaped part was produced via plunger-type injection moulding. The green part was sintered at 1000, 1100, 1200 and 1300°C at 3 hours. The value of flow behaviour index n is from 0·1 to 0·39, which is within range of the injectability index. The obtained activation energy is 5·75 kJ mol^{-1}. Morphological results indicate the formation of pores at a sintering temperature of 1000°C, a decrease of pores when the temperature is increased, and the occurrence of densification. At 1300°C it showed the highest mechanical properties of Young's modulus which is 41·18 GPa. The decomposition of hydroxyapatite into β-tricalcium phosphate and tetracalcium phosphate phases started to occur at 1000 and 1100°C, respectively. The highest sintered density is 3·7744 g cm^{-3} which is close to the density of hydroxyapatite but the mechanical properties is higher than pure hydroxyapatite.

Keywords: Powder injection moulding, Hydroxyapatite–stainless steel 316L composite, Rheological properties, Physical properties

Introduction

Powder injection moulding (PIM) is a technological process used to manufacture metal and ceramic and can produce small, complex, precise and net-shaped components at a competitive cost.[1] Powder injection moulding consists of four main steps, namely mixing, injection moulding, debinding and sintering.

Hydroxyapatite (HA) is a calcium phosphate ceramic whose structure and composition are similar to that of human bones and teeth.[2,3] Hydroxyapatite is widely used as a bone substitute and dental implant because of its good properties, such as high biocompatibility, osseoconductivity and bioaffinity with living tissues.[2,4,5] However, HA has low mechanical properties, such as brittleness and low fracture toughness, which limit its use in load-bearing applications.[6] Therefore, metallic materials are used to improve the mechanical properties of metal–ceramic composites.

Stainless steel 316L (SS 316L), cobalt–chromium alloys (Co–Cr–Mo), titanium (Ti) and titanium alloys (Ti–6Al–4 V) are metallic materials that are widely used as implant materials, especially in the fields of orthopaedics and dentistry.[7,8] These materials are used because of their good mechanical properties, corrosion resistance and the formation of an inert biocompatible oxide layer on their surface. As one of the medical grade metals used in implants, SS 316L is a well-known alloy that is suitable for use in internal fixation devices.[9] Stainless steel 316L is traditionally used because it is low cost, easy to fabricate and possesses high mechanical properties. Properties such as corrosion resistance, biocompatibility, high tensile strength and fatigue resistance make SS 316L suitable as a surgical implant material.[10]

The combination of the excellent strength properties of SS 316L and the bioceramics of HA can be used in load-bearing applications and bioactive composites.[11]

[1]Department of Mechanical and Materials Engineering, Faculty of Engineering and Built Environment, Universiti Kebangsaan Malaysia, 43600 Bangi, Selangor, Malaysia
[2]Department of Mechanical Engineering, Sriwijaya University, 30662 Indralaya, Sumatera Selatan, Indonesia

*Corresponding author, email mohdikram151@gmail.com

Furthermore, the thermal expansion coefficient of SS 316L is close to that of HA ceramics.[12,13] In recent years, much research has been conducted on the fabrication techniques of SS 316L–HA composites, including compressing technique, surface modification, coating, spark plasma sintering and compression,[14–17] but few studies have been reported on the PIM process. The use of palm stearin (PS) and polyethylene (PE) as a binder system was successfully studied through a single material by Mohd Foudzi *et al.*,[18] Omar *et al.*[19] and Nor *et al.*[20] but less reported using two different materials composite. In this study, the emphasis on the use of PS and PE in SS 316L/HA feedstock were determined.

The objectives of this study were to evaluate the reliability of the use of PS and PE as a binder system and to characterise the sintered part of the composite. The following rheological properties of the SS 316L–HA feedstock were measured: flow rate, shear rate and activation energy. The sintered parts were analysed on the physical and mechanical properties based on the different sintering temperatures. The scope of this study used 58·0 vol.-% powder loading feedstock of 50 wt-% SS 316 and 50 wt-% HA.

Materials and methods

The powder was prepared by mixing 50 wt-% of SS 316L powder, purchased from Epson Atmix Corporation, with 50 wt-% of HA, supplied by Sigma Aldrich (M) Sdn. Bhd. The sizes (D_{50}) of the powders were 6·75 and 5·34 μm, respectively. About 60 wt-% PS and 40 wt-% PE were mixed together with the powder by using a Brabender mixer at 150°C to form a binder system.[21–23] A feedstock of 58·0 vol.-% powder loading was produced. The rheological characteristics of the feedstock were measured using the Shimadzu CFT-500D capillary rheometer at 150, 160, 170 and 180°C.

The feedstock was injected using a DSM Explore plunger-type injection moulding machine with a green dumbbell-shaped part. Two stages of the thermal debinding process were conducted at 320 and 500°C to remove the binder system. This temperature was successfully reported by Mohd Foudzi *et al.*[18] and Omar *et al.*[19] which is the decomposition of PS and PE occurs at 300 and 450°C, respectively.

The debound parts were sintered at 1000, 1100, 1200 and 1300°C for 3 hours of holding time at a heating rate of 3°C per minute, based on the conditions used in previous studies of Salman *et al.*[24] and Ruys *et al.*[25] The morphology were characterised via scanning electron microscopy (Hitachi model S3400N SEM) and the density of sintered samples were measured by using an electronic balance (Sartorus, model BSA224S-CW) based on MPIF Standard 42.[26] The Young's modulus properties were examined using a Universal Testing Machine (model 5567) and follow the test method of MPIF Standard 41.[26] All sampels were tested by X-ray diffraction (XRD) using the XRD Bruker D8 Advance with a CuKα irradiation to determine the phase present at all temperatures.

Results and discussion

The behaviour of a PIM feedstock is generally considered to be similar to that of pseudoplastic fluids, the viscosity of which decreases with increasing shear rate. This behaviour can be defined based on the power law equation[27]

$$\eta = K\gamma^{n-1} \tag{1}$$

where η is the viscosity, K is a constant, γ is the shear rate and n is the index of flow behaviour for the feedstock. In the PIM process, the value of viscosity must be lower than 1000 Pa s and the shear rate must be between 100 and 100 000 per second.[28] Figure 1 shows that 58 vol.-% feedstock demonstrates pseudoplastic behaviour and is suitable for injection moulding. The determined n values are $n_{150} = 0{\cdot}24$, $n_{160} = 0{\cdot}39$, $n_{170} = 0{\cdot}26$ and $n_{180} = 0{\cdot}10$. The highest obtained value is 0·39. All n values are within the pseudoplastic range ($n < 1$). The correlation between the viscosity and temperature describes the flow activation energy E of the feedstock through the Arrhenius equation[27]

$$\eta = \eta_o \exp(E/RT) \tag{2}$$

where η_o is the viscosity at a reference temperature, E is the flow activation energy, R is the gas constant and T is the temperature. The flow activation energy can be determined by the slope of $\ln \eta$ *v.* $1/T$ graph.[29] A large value of E shows the high sensitivity of viscosity to changes in temperature.

In Fig. 2, the graph was plotted based on loads of 100, 120, 130 and 140 N applied to the feedstock. The following values of E were obtained: $E_{100} = 12{\cdot}74$ kJ mol^{-1}, $E_{120} = 26{\cdot}0$ kJ mol^{-1}, $E_{140} = 5{\cdot}75$ kJ mol^{-1} and $E_{160} = 9{\cdot}42$ kJ mol^{-1}. E_{140} had the smallest activation energy, followed by E_{160}, E_{100} and E_{120}. However, all values of the activation energy are still considerably low when compared with the values obtained in many previous studies on rheology.[22,23,27,30] The oil and fats in PS can form a lubricant film, which decreases the viscosity and increases the activation energy of the feedstock. Iriany *et al.* stated that the concentration of PS in the binder must not be more than 45 wt-% to prevent the powder binder separation phenomenon.[31]

Morphological studies on the sintered sample were conducted via SEM to study the distribution and dispersion of both SS 316L and HA powder. The samples sintered at 1000°C (Fig. 3*a*), 1100°C (Fig. 3*b*) and 1200°C (Fig. 3*c*) exhibited high porosity compared with

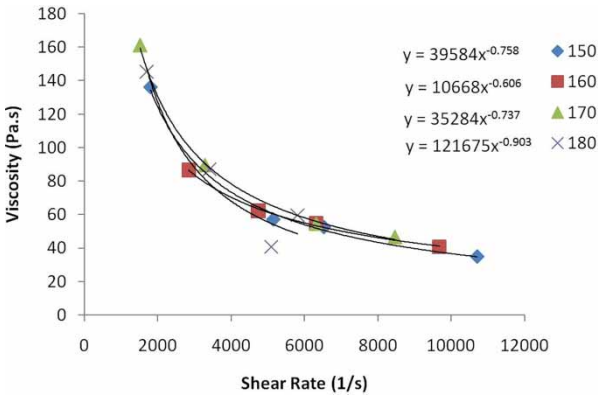

1 Graph of relation between viscosity and shear rate at 150, 160, 170 and 180°C

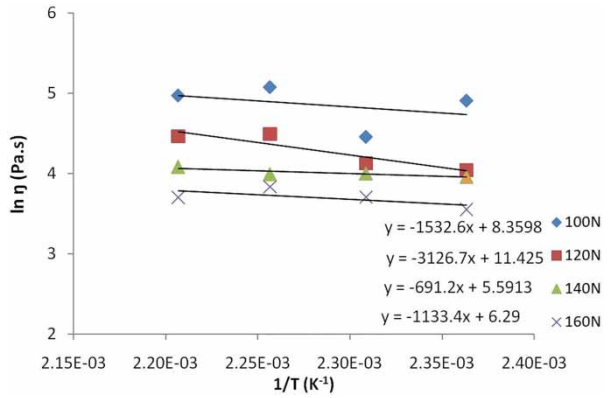

2 Correlation between viscosity and temperature for 58·0 vol.-% feedstock

those sintered at 1300°C (Fig. 3*d*). Densification did not occur until the sintering temperature was increased to 1300°C. Grain growth, as well as densification, increased with increasing temperature, a result similar to those obtained by Song *et al.*[32] and Muralithran and Ramesh.[33]

The SEM image shows that the HA was well sintered at 1300°C. By contrast, the SS 316L was not properly diffused. This phenomenon occurred because no contact point was made between the SS 316L particles, which were far apart from one another. The pore sizes decreased and tended to disappear, and the shape became more 'rounded' with increasing temperature. This result was supported by previous studies of Prokopiev and Sevostianov,[34] and Olevsky.[35]

The final densities of all samples were measured after the sintering process completed. The sintered densities of each temperature were measured to four decimal points. The sintered sample at 1300°C (Fig. 3*d*) shows the highest density of 3·7744 g cm^{-3} which is 83·4% close to the theoretical value. Followed by 1200°C (3·6846 g cm^{-3}), 1100°C (3·6264 g cm^{-3}) and 1000°C (3·5920 g cm^{-3}). This happened owing to the presence of voids; the density increased with decreasing number of voids.[18] At 1300°C, the sample was observed to have the least amount of voids compared to 1200, 1100 and 1000 °C. The results were supported by Prokopiev and Sevostianov[34] in his research that the density increases because the pores tend to coalescence which their number decreases as the temperature continues to grow.

Young's modulus for all sintered samples was determined based on three-point bending test. As the sintering temperature elevates, Young's modulus increases. The sintered sample at 1300°C had the highest Young's modulus which is 41·18 GPa followed by 1200°C (34·84 GPa), 1100°C (27·53 GPa) and 1000°C (22·74 GPa). By comparing with the density results, it is found that the Young's modulus increases because of the densification as a result of sufficient diffusion bond formed between the particles. Neuendorf *et al.*,[36] Lee *et al.*[37] and Arifin *et al.*[38] stated that the mechanical properties of bone for Young's modulus are between 10 and 30 GPa. It shows that the strength of Young's modulus of the composites SS316L/HA is exceeded the strength of the bone caused by the inclusion of SS316L.

Based on the XRD result in Fig. 4, the decomposition of HA into β-tricalcium phosphate (β-TCP), $Ca_3(PO_4)_2$ occurred at the following temperatures: 1000, 1100, 1200 and 1300°C. The amount of β-TCP phase increased with increasing temperature. At 1100°C and above, the HA also decomposed into tetracalcium phosphate (TTCP), $Ca_4(PO_4)_2O$. The SS 316L did not change into other phases at any sintering temperature.

The decomposition of HA occurred as a result of the formation of an intermediate phase, oxyapatite, $Ca_{10}(PO_4)_6O$ which was formed via the dehydrolation process, when HA was sintered in air at temperature

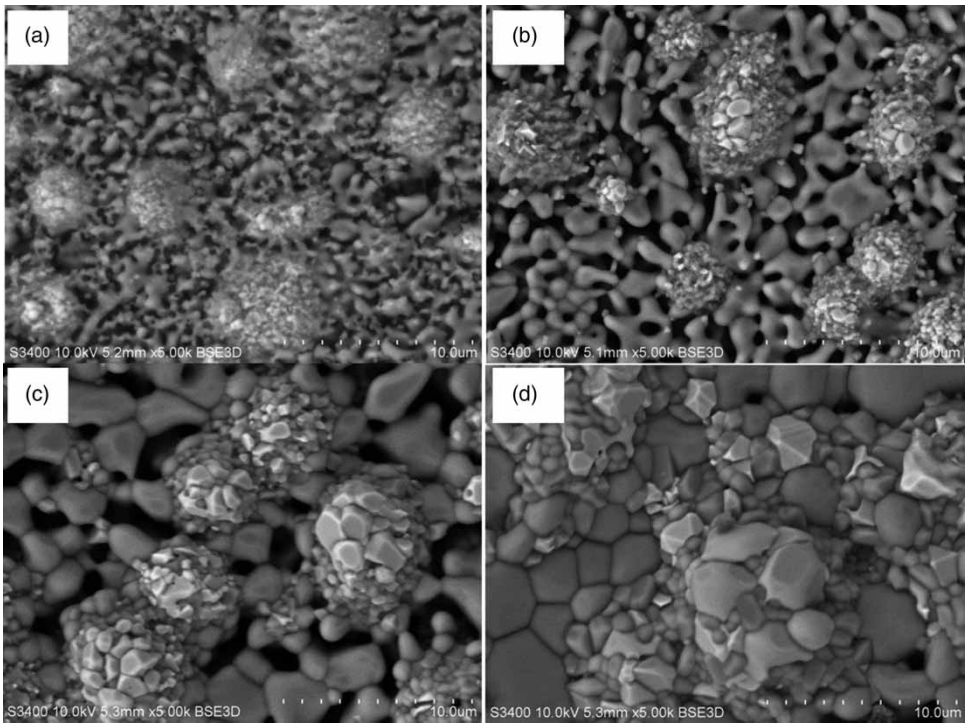

3 SEM image of sintered 58·0 vol.-% *a* 1000°C, *b* 1100°C, *c* 1200°C and *d* 1300°C

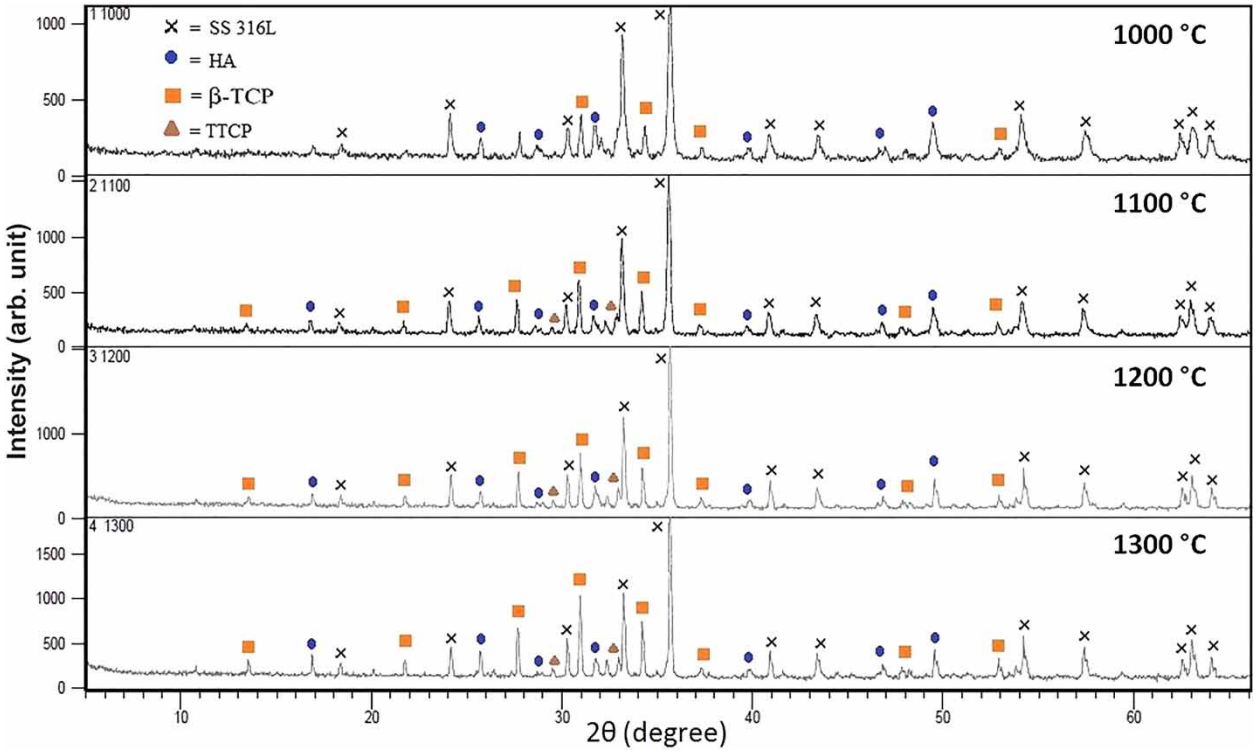

4 X-ray diffraction patterns of sintered part for 3 hours at 1000, 1100, 1200 and 1300°C

above 1200°C.[33] Zhou *et al.*[39] stated that during the sintering process, H_2O is produced and the formation of oxyapatite occurs based on the following equations:

$$2OH \rightarrow O + H_2O \uparrow \quad (3)$$

$$Ca_{10}(PO_4)_6(OH)_2 \rightarrow Ca_{10}(PO_4)_6O + H_2O \quad (4)$$

This oxyapatite phase is stable and does not undergo any reverse phase transformation. However, the decomposition of HA into β-TCP and TTCP occurs if further heating is applied based on the following equation:[39]

$$Ca_{10}(PO_4)_6(OH)_2 \rightarrow 2Ca_3(PO_4)_2 + Ca_4(PO_4)_2O + H_2O \quad (5)$$

In their previous research, Wang and Chaki[40] reported that HA decomposes into another phase at a lower temperature through the dehydration process if the sintering time takes longer than 2 hours.

Conclusion

The stainless steel 316L–hydroxyapatite composite was successfully fabricated using palm stearin and polyethylene as a binder system. The rheological results showed that the feedstock of 58 vol.-% powder loading exhibited pseudoplastic behaviour with viscosity <1000 Pa s and shear rate was between 100 and 10 000 s^{-1}. The injectability indices were within the range of $-1 < n < 1$. The obtained lowest activation energy, $E = 5{\cdot}75$ kJ mol^{-1}, indicated less sensitivity to temperature change. Pores were formed during the sintering process and their sizes decreased when the sintering temperature was increased. The mechanical properties increased with temperature increased. At 1300°C, dense hydroxyapatite was observed and the highest density obtained which is 83·4% close to theoretical value. The same trend measured to the highest value of Young's modulus of 41·18 GPa which already surpasses the limit of human bone. The decomposition of hydroxyapatite into β-tricalcium phosphate and tetracalcium phosphate starts at sintering temperatures of 1000 and 1100°C, respectively. Good physical and mechanical properties of stainless steel 316L–hydroxyapatite composite can be achieved by using higher powder loading of stainless steel 316L/hydroxyapatite feedstock.

Acknowledgements

The authors express their sincere thanks and appreciation to the Malaysia Ministry of Education and Universiti Kebangsaan Malaysia for their financial support under grants FRGS/2/2013/TK01/UKM/02/3 and ERGS/1/2012/TK01/UKM/02/1.

References

1. S. Ahn, S. J. Park, S. Lee, S. V. Atre and R. M. German: 'Effect of powders and binders on material properties and molding parameters in iron and stainless steel powder injection molding process', *Powder Technol.*, 2009, **193**, (2), 162–169.
2. J. M. Cordell, M. L. Vogl and A. J. Wagoner Johnson: 'The influence of micropore size on the mechanical properties of bulk hydroxyapatite and hydroxyapatite scaffolds', *J. Mech. Behav. Biomed.*, 2009, **2**, (5), 560–570.
3. M. Mihailovic, A. Pataric, Z. Gulisija, D. Veljovic and D. Janackovic: 'Electrophoretically deposited nanosized hydroxyapatite coatings on 316lvm stainless steel for orthopaedic implants', *Chem. Ind. Chem. Eng. Q*, 2011, **17**, (1), 45–52.
4. M. Javidi, S. Javadpour, M. E. Bahrololoom and J. Mia: 'Electrophoretic deposition of natural hydroxyapatite on medical grade 316L stainless steel', *Mater. Sci. Eng. C*, 2008, **28**, (8), 1509–1515.

5. F. Daitou, M. Maruta, G. Kawachi, K. Tsuru, S. Matsuya, Y. Terada and K. Ishikawa: 'Fabrication of carbonate apatite block based on internal dissolution-precipitation reaction of dicalcium phosphate and calcium carbonate', *Dent. Mater. J.*, 2010, **29**, (3), 303–308.
6. X. Fan, J. Chen, J. P. Zou, Q. Wan, Z. C. Zhou and J. M. Ruan: 'Bone-like apatite formation on HA/316L stainless steel composite surface in simulated body fluid', *T. Nonferr. Metal. Soc.*, 2009, **19**, (2), 347–352.
7. F. A. Azem and A. Cakir: 'Synthesis of HAP coating on galvanostatically treated stainless steel substrates by sol–gel method', *J. Sol–Gel Sci. Technol.*, 2009, **51**, (2), 190–197.
8. M. C. D. Andrade, M. R. Tavares Filgueiras and T. Ogasawara: 'Hydrothermal nucleation of hydroxyapatite on titanium surface', *J. Eur. Ceram. Soc.*, 2002, **22**, (4), 505–510.
9. L. Hao, J. Lawrence, Y. F. Phua, K. S. Chian, G. C. Lim and H. Y. Zheng: 'Enhanced human osteoblast cell adhesion and proliferation on 316 LS stainless steel by means of CO_2 laser surface treatment', *J. Biomed. Mater. Res. B*, 2005, **73B**, (1), 148–156.
10. K. B. Devi, K. Singh and N. Rajendran: 'Sol–gel synthesis and characterisation of nanoporous zirconium titanate coated on 316L SS for biomedical applications', *J. Sol–Gel Sci. Technol.*, 2011, **59**, (3), 513–520.
11. L. Hao, S. Dadbakhsh, O. Seaman and M. Felstead: 'Selective laser melting of a stainless steel and hydroxyapatite composite for load-bearing implant development', *J. Mater. Process. Technol.*, 2009, **209**, (17), 5793–5801.
12. X. Miao, A. J. Ruys and B. K. Milthorpe: 'Hydroxyapatite-316L fibre composites prepared by vibration assisted slip casting', *J. Mater. Sci.*, 2001, **36**, (13), 3323–3332.
13. R. Rogier and F. Pernot: 'Glass–ceramic–metal composites for making graded seals in prosthetic devices', *J. Mater. Sci. Mater. Med.*, 1991, **2**, (3), 153–161.
14. H. B. Guo, X. Miao, Y. Chen, P. Cheang and K. A. Khor: 'Characterization of hydroxyapatite- and bioglass-316L fibre composites prepared by spark plasma sintering', *Mater. Lett.*, 2004, **58**, (3–4), 304–307.
15. J. Gallardo, P. Galliano and A. Duran: 'Bioactive and protective sol–gel coatings on metals for orthopaedic prostheses', *J. Sol–Gel Sci. Technol.*, 2001, **21**, (1–2), 65–74.
16. J. P. Zou, J. M. Ruan, B. Y. Huang, J. B. Liu and X. X. Zhou: 'Physico-chemical properties and microstructure of hydroxyapatite-316L stainless steel biomaterials', *J. Cent. South Univ. T*, 2004, **11**, (2), 113–118.
17. L. Pramatarova, E. Pecheva and V. Krastev: 'Ion implantation modified stainless steel as a substrate for hydroxyapatite deposition. Part I. Surface modification and characterization', *J. Mater. Sci. Mater. Med.*, 2007, **18**, (3), 435–440.
18. F. Mohd Foudzi, N. Muhamad, A. B. Sulong and H. Zakaria: 'Yttria stabilized zirconia formed by micro ceramic injection molding: Rheological properties and debinding effects on the sintered part', *Ceram. Int.*, 2013, **39**, (3), 2665–2674.
19. M. A. Omar, I. Subuki, N. S. Abdullah, N. M. Zainon and N. Roslani: 'Processing of water-atomised 316L stainless steel powder using metal-injection process', *J. Eng. Sci.*, 2012, **8**, 1–13.
20. N. H. M. Nor, N. Muhamad, M. H. Ismail, K. R. Jamaludin, S. Ahmad and M. H. I. Ibrahim: 'Injection molding parameter optimization of titanium alloy powder mix with palm stearin and polyethylene for green defects using taguchi method', 3rd Powder Metallurgy Symposium and Exhibition, Kuala Lumpur; 2010, s85–87.
21. N. Muhamad, N. H. M. Nor, S. Ahmad, M. H. I. Ibrahim and M. R. Harun: 'Multiple performance optimization for the best injection molding process of Ti–6Al–4 V green compact', *Appl. Mech. Mater.*, 2010, **44–47**, 2707–2711.
22. M. R. Harun, N. Muhamad, A. B. Sulong, N. H. M. Nor and M. H. I. Ibrahim: 'Rheological investigation of ZK60 magnesium alloy feedstock for metal injection moulding using palm stearin based binder system', *Front. Manufacturing Des. Sci.*, 2011, **44–47**, (Pts 1–4), 4126–4130.
23. M. F. Abdullah, A. B. Sulong, N. Muhamad, M. I. H. C. Abdullah and N. H. N. Yahya: 'Comparison on rheology properties of polypropylene and polyethylene as binder system with stainless steel 316L for metal injection moding', *Compos. Sci. Technol.*, 2011, **471–472**, (Pts 1 and 2), 409–414.
24. S. Salman, O. Gunduz, S. Yilmaz, M. L. Ovecoglu, R. L. Snyder, S. Agathopoulos and F. N. Oktar: 'Sintering effect on mechanical properties of composites of natural hydroxyapatites and titanium', *Ceram. Int.*, 2009, **35**, (7), 2965–2971.
25. A. J. Ruys, M. Wei, C. C. Sorrell, M. R. Dickson, A. Brandwood and B. K. Milthorpe: 'Sintering effects on the strength of hydroxyapatite', *Biomaterials*, 1995, **16**, (5), 409–415.
26. MPIF, 'Standard test methods for metal powders and powder metallurgy products'; 2006, Princeton, NJ, Metal Powder Industries Federation.
27. M. A. Omar, I. Subuki, N. S. Abdullah and M. F. Ismail: 'The influence of palm stearin content on the rheological behavior of 316L stainless steel MIM compact', *J. Sci. Technol.*, 2010, **2**, (2), 1–14.
28. R. M. German and A. Bose: 'Injection molding of metals and ceramics'; 1997, Princeton, NJ, Metal Powder Industry Federation.
29. H. Abolhasani and N. Muhamad: 'A new starch-based binder for metal injection molding', *J. Mater. Process. Technol.*, 2010, **210**, (6–7), 961–968.
30. B. Huang, S. Liang and X. Qu: 'The rheology of metal injection molding', *J. Mater. Process. Technol.*, 2003, **137**, (1–3), 132–137.
31. Iriany: 'Development of binder formulation in metal injection molding'; 2002, Bangi, Selangor, Department of Mechanics and Materials, Universiti Kebangsaan Malaysia.
32. J. Song, Y. Liu, Y. Zhang and L. Jiao: 'Mechanical properties of hydroxyapatite ceramics sintered from powders with different morphologies', *Mater. Sci. Eng. A*, 2011, **528**, (16–17), 5421–5427.
33. G. Muralithran and S. Ramesh: 'The effects of sintering temperature on the properties of hydroxyapatite', *Ceram. Int.*, 2000, **26**, (2), 221–230.
34. O. Prokopiev and I. Sevostianov: 'Dependence of the mechanical properties of sintered hydroxyapatite on the sintering temperature', *Mater. Sci. Eng. A*, 2006, **431**, (1–2), 218–227.
35. E. A. Olevsky: 'Theory of sintering: from discrete to continuum', *Mater. Sci. Eng. R*, 1998, **23**, (2), 41–100.
36. R. E. Neuendorf, E. Saiz, A. P. Tomsia and R. O. Ritchie: 'Adhesion between biodegradable polymers and hydroxyapatite: relevance to synthetic bone-like materials and tissue engineering scaffolds', *Acta Biomater.*, 2008, **4**, (5), 1288–1296.
37. S. Lee, M. Porter, S. Wasko, G. Lau, P. Y. Chen, E. E. Novitskaya, A. P. Tomsia, A. Almutairi, M. A. Meyers and J. McKittrick: 'Potential bone replacement materials prepared by two methods', *Mater. Res. Soc. Symp. P*, 2012, **1418**, 177–188.
38. A. Arifin, A. B. Sulong, N. Muhamad, J. Syarif and M. I. Ramli: 'Material processing of hydroxyapatite and titanium alloy (HA/Ti) composite as implant materials using powder metallurgy: a review', *Mater. Des.*, 2014, **55**, 165–175.
39. J. Zhou, X. Zhang, J. Chen, S. Zeng and K. Groot: 'High temperature characteristics of synthetic hydroxyapatite', *J. Mater. Sci. Mater. Med.*, 1993, **4**, (1), 83–85.
40. P. Wang and T. K. Chaki: 'Sintering behaviour and mechanical properties of hydroxyapatite and dicalcium phosphate', *J. Mater. Sci. Mater. Med.*, 1993, **4**, (2), 150–158.